

Prospects for constraining interacting dark energy model with 21 cm intensity mapping experiments

Ming Zhang,¹ Bo Wang,¹ Jing-Zhao Qi,¹ Yidong Xu,^{2,*} Jing-Fei Zhang,¹ and Xin Zhang^{1,†}

¹*Department of Physics, College of Sciences, & MOE Key Laboratory of Data Analytics and Optimization for Smart Industry, Northeastern University, Shenyang 110819, China*

²*National Astronomical Observatories, Chinese Academy of Sciences, Beijing 100101, China*

We forecast the constraints on cosmological parameters in the interacting dark energy model using the mock data generated for neutral hydrogen intensity mapping (IM) experiments. In this work, we consider only the interacting dark energy model with the energy transfer rate $Q = \beta H \rho_c$, and take BINGO, FAST, SKA1-MID, and Tianlai as typical examples of the 21 cm IM experiments. We find that the Tianlai cylinder array will play an important role in constraining the interacting dark energy model. Assuming perfect foreground removal and calibration, and using the Tianlai-alone data, we obtain $\sigma(H_0) = 0.10 \text{ km s}^{-1} \text{ Mpc}^{-1}$, $\sigma(\Omega_m) = 0.0013$, and $\sigma(\sigma_8) = 0.0015$ in the Λ CDM model, which are much better than the results of Planck+optical BAO (i.e. optical galaxy surveys). However, the Tianlai-alone data cannot provide very tight constraint on the coupling parameter β , compared with Planck+optical BAO, while the Planck+Tianlai data can give a rather tight constraint of $\sigma(\beta) = 0.00052$, due to the parameter degeneracies being well broken by the data combination. In the Iw CDM model, we obtain $\sigma(\beta) = 0.00058$ and $\sigma(w) = 0.006$ from Planck+Tianlai. In addition, we also make a detailed comparison among BINGO, FAST, SKA1-MID, and Tianlai in constraining the interacting dark energy model. We show that the future 21 cm IM experiments will provide a useful tool for exploring the nature of dark energy, and will play a significant role in measuring the coupling between dark energy and dark matter.

I. INTRODUCTION

According to our understanding to the contemporary cosmology, dark energy is responsible for the accelerating expansion of the universe [1]. Until now, however, the nature of dark energy still remains a deep mystery. To explore dark energy in depth and also to test the possible deviation from General Relativity, it is necessary to precisely measure the late-time expansion history of the universe. Among the several ways of exploring the cosmic expansion history, the baryon acoustic oscillations (BAO) [2, 3] have been proven to be a very useful tool to measure cosmological distance and Hubble expansion rate and to explore the nature of dark energy. Because the acoustic waves are frozen in the eras after recombination, the BAO peak wavelengths, as a cosmological standard ruler, allows accurate measurements of the expansion history.

Galaxy surveys could achieve a tomography of the universe over its last twelve billion years. In addition, due to the hyperfine transition of neutral hydrogen (HI) at 21 cm wavelength, via 21 cm emission, BAO signals could be precisely measured [4]. HI is essentially a tracer of the galaxy distribution. Detecting a sufficiently large number of galaxies with HI 21 cm emission could make it possible to provide a useful tool for cosmological research, but actually it is unnecessary to perform a galaxy survey for the study of large-scale structure. We can instead measure the total HI intensity over large angular scales,

without needing to resolve individual galaxies. Similar to the cosmic microwave background (CMB) map, this intensity mapping (IM) methodology makes it possible to efficiently survey large volumes with modern radio telescopes [5–28].

Using the HI IM method, Chang et al. [29] reported the measurements of cross-correlation function between the HI map observed with the Green Bank Telescope (GBT) and the galaxy map with the DEEP2 optical redshift survey. The cross-power spectrum between HI and optical galaxy survey was also detected with the GBT 21 cm IM survey and the WiggleZ Dark Energy Survey [30]. Lately, Anderson et al. [31] reported the results from 21 cm IM acquired from the Parkes radio telescope and cross-correlated with galaxy maps from the 2dF galaxy survey. So far, there are many current and future HI IM experiments comprised of wide-field and high-sensitivity radio telescopes or interferometers. Here we consider several typical examples, namely, the Baryon acoustic oscillations In Neutral Gas Observations (BINGO) [6, 32–34], the Five-hundred-meter Aperture Spherical radio Telescope (FAST) [35–40], the Square Kilometre Array (SKA) [24, 41–43], and the Tianlai cylinder array [18, 44–48]. This work aims to forecast how future HI IM experiments, including BINGO, FAST, SKA Phase I mid-frequency array (SKA1-MID), and Tianlai, can constrain the interacting dark energy (IDE) model.

The IDE model originates from a longstanding conjecture that there might be some coupling between dark energy (DE) and cold dark matter (CDM) (for a recent review, see Ref. [49]). The model with an interaction between vacuum energy (for convenience, dark energy with $w = -1$ is called the vacuum energy in this work, and is denoted by Λ) and CDM is usually called the Λ CDM

* xuyd@nao.cas.cn

† zhangxin@mail.neu.edu.cn

model. Besides, we also wish to consider the more general IDE model in which the dark-energy equation of state (EoS) parameter w is a constant, usually called the Iw CDM model. In the Iw CDM scenario, the energy conservation equations for DE and CDM satisfy

$$\dot{\rho}_{\text{de}} = -3H(1+w)\rho_{\text{de}} + Q, \quad (1)$$

$$\dot{\rho}_{\text{c}} = -3H\rho_{\text{c}} - Q, \quad (2)$$

where Q is the energy transfer rate, ρ_{de} and ρ_{c} denote the energy densities of DE and CDM, respectively, $H = \dot{a}/a$ represents the Hubble parameter, a is the scale factor of the universe, and a dot represents the derivative with respect to the cosmic time t . Here the case of $w = -1$ corresponds to the Λ CDM model. Many specific forms for Q have been constructed and discussed in previous works [50–84]. In this paper, we employ a phenomenological form of $Q = \beta H\rho_{\text{c}}$, where β denotes a dimensionless coupling parameter. From Eqs. (1) and (2), it can be seen that $\beta > 0$ indicates that CDM decays into DE, $\beta < 0$ indicates that DE decays into CDM, and $\beta = 0$ means that there is no interaction between DE and CDM.

In this work, we study what role the 21 cm IM experiments would play in constraining cosmological parameters in the Λ CDM and Iw CDM models. Combining with the Planck CMB data [85], we wish to forecast how these 21 cm IM experiments will improve the constraints on cosmological parameters. We also make a comparison with optical galaxy surveys. Unless otherwise stated, we employ the spatially-flat Λ CDM model with parameters fixed by fitting to the Planck 2018 data [85] as a fiducial model to generate mock data.

This paper is organized as follows. In Section II, we give a detailed description of methodology. In Section II A, we introduce signal power spectrum and noise power spectrum of the 21 cm IM experiments, and construct the Fisher matrix. We further give a detailed description of the experimental configurations in Section II B, and describe methods and data employed in this paper in Section II C. In Section III, we present forecasted constraints on cosmological parameters and make some relevant discussions. Finally, we give our conclusions in Section IV.

II. METHODOLOGY

A. 21 cm intensity mapping

The mean HI brightness temperature is given by (the detailed derivation can be found in Ref. [6])

$$\bar{T}_b(z) = 180\Omega_{\text{HI}}(z)h \frac{(1+z)^2}{H(z)/H_0} \text{ mK}, \quad (3)$$

where $\Omega_{\text{HI}}(z)$ is the fractional density of HI, $H(z)$ is the Hubble parameter as a function of redshift z , $H_0 \equiv 100h \text{ km s}^{-1} \text{ Mpc}^{-1}$ is its value today, and h is the dimensionless Hubble constant. Considering the effect of

redshift space distortions (RSD) [86], the signal HI power spectrum can be written as [3]

$$P^S(k_{\text{f}}, \mu_{\text{f}}, z) = \bar{T}_b^2 \frac{D_{\text{A}}(z)_{\text{f}}^2 H(z)_{\text{f}}}{D_{\text{A}}(z)^2 H(z)_{\text{f}}} b_{\text{HI}}^2 [1 + \beta_{\text{HI}}(z)\mu^2]^2 P(k, z), \quad (4)$$

where the subscript “f” denotes the quantities calculated in the fiducial cosmology, D_{A} is the angular diameter distance, b_{HI} is the HI bias, $\mu = \hat{k} \cdot \hat{z}$, β_{HI} is the RSD parameter equal to f/b_{HI} ($f \equiv d\ln D/d\ln a$ is the linear growth rate with a being the scale factor) in linear theory, and $P(k, z) = D^2(z)P(k, z=0)$, with $D(z)$ being the growth factor and $P(k, z=0)$ being the matter power spectrum at $z=0$ that can be generated by CAMB [87]. Note here that the “Fingers of God” (FoG) effect due to uncorrelated peculiar velocities on small scales is ignored in this work.

The noise power spectrum models the instrumental and sky noises for a given experiment. The survey noise properties have been described in detail in Refs. [6, 17]. Here, we summarize them for completeness. The frequency resolution of IM surveys performs well, so we ignore the instrument response function in the radial direction and only consider the response due to the finite angular resolution:

$$W^2(k) = \exp \left[-k_{\perp}^2 r^2(z) \left(\frac{\theta_{\text{B}}}{\sqrt{8\ln 2}} \right)^2 \right], \quad (5)$$

where k_{\perp} is the transverse wave vector, $r(z)$ is the comoving radial distance at redshift z , and θ_{B} is the full width at half-maximum of the beam of an individual dish.

If considering a redshift bin between z_1 and z_2 , the survey volume can be written as

$$V_{\text{sur}} = \Omega_{\text{tot}} \int_{z_1}^{z_2} dz \frac{dV}{dz d\Omega} = \Omega_{\text{tot}} \int_{z_1}^{z_2} dz \frac{cr^2(z)}{H(z)}, \quad (6)$$

where $\Omega_{\text{tot}} = S_{\text{area}}$ is the solid angle of the survey area. The pixel volume V_{pix} is also calculated with the similar formula with Ω_{tot} substituted by $\Omega_{\text{pix}} \approx \theta_{\text{B}}^2$.

For an experiment using single-dish mode, the pixel noise can be written as

$$\sigma_{\text{pix}} = \frac{T_{\text{sys}}}{\sqrt{\Delta\nu t_{\text{tot}} (\theta_{\text{B}}^2/S_{\text{area}})}} \frac{\lambda^2}{A_{\text{e}} \theta_{\text{B}}^2} \frac{1}{\sqrt{N_{\text{dish}} N_{\text{beam}}}}, \quad (7)$$

and for an interferometer, the pixel noise can be written as

$$\sigma_{\text{pix}} = \frac{T_{\text{sys}}}{\sqrt{\Delta\nu t_{\text{tot}} (\text{FoV}/S_{\text{area}})}} \frac{\lambda^2}{A_{\text{e}} \sqrt{\text{FoV}}} \frac{1}{\sqrt{n(k_{\perp}) N_{\text{beam}}}}, \quad (8)$$

where T_{sys} is the system temperature, N_{dish} is the number of dishes and N_{beam} is the number of beams, t_{total} is the total observing time, A_{e} is the effective collecting area of each element. For a dish reflector, $A_{\text{e}} \equiv$

$\eta\pi(D_{\text{dish}}/2)^2$ and $\theta_B \approx \lambda/D_{\text{dish}}$, where D_{dish} is the diameter of the dish, and η is an efficiency factor for which we adopt 0.7 in this work. For a cylindrical reflector, $A_e \equiv \eta l_{\text{cyl}} w_{\text{cyl}}/N_{\text{feed}}$ and $\text{FoV} \approx 90^\circ \times \lambda/w_{\text{cyl}}$, where w_{cyl} and l_{cyl} are width and length of cylinder, respectively, and N_{feed} is the number of feeds per cylinder. Unlike a single dish, we need to calculate the baseline density $n(k_\perp)$ for the interferometer. The detailed calculation method can be found in Ref. [17].

For BINGO, FAST, and Tianlai, the system temperature is given by

$$T_{\text{sys}} = T_{\text{rec}} + T_{\text{gal}} + T_{\text{CMB}}, \quad (9)$$

where T_{rec} is the receiver temperature for each of these experiments with the values given in Table I, $T_{\text{gal}} \approx 25 \text{ K}(408 \text{ MHz}/\nu)^{2.75}$ is the contribution from the Milky Way for a given frequency ν , and $T_{\text{CMB}} \approx 2.73 \text{ K}$ is the CMB temperature. For the SKA1-MID array, the system temperature is calculated by

$$T_{\text{sys}} = T_{\text{rec}} + T_{\text{spl}} + T_{\text{gal}} + T_{\text{CMB}}, \quad (10)$$

where $T_{\text{spl}} \approx 3 \text{ K}$ is the contribution from spill-over. The receiver temperature T_{rec} for SKA1-MID is assumed to be [88]

$$T_{\text{rec}} = 15 \text{ K} + 30 \text{ K} \left(\frac{\nu}{\text{GHz}} - 0.72 \right)^2. \quad (11)$$

Finally, the noise power spectrum is then given by

$$P^N(k) = \sigma_{\text{pix}}^2 V_{\text{pix}} W^{-2}(k). \quad (12)$$

The Fisher matrix for a set of parameters $\{p\}$ is given by [89]

$$F_{ij} = \frac{1}{8\pi^2} \int_{-1}^1 d\mu \int_{k_{\text{min}}}^{k_{\text{max}}} k^2 dk \frac{\partial \ln P^S}{\partial p_i} \frac{\partial \ln P^S}{\partial p_j} V_{\text{eff}}, \quad (13)$$

where we define the “effective volume” as [17, 19]

$$V_{\text{eff}} = V_{\text{sur}} \left(\frac{P^S}{P^S + P^N} \right)^2. \quad (14)$$

Next, we assume that the bias b_{HI} depends only on the redshift z . This assumption is appropriate only for large scales, so we impose a non-linear cut-off at $k_{\text{max}} \simeq 0.14(1+z)^{2/3} \text{ Mpc}^{-1}$ [90]. Hence, we ignore the small-scale velocity dispersion effect of FoG (parameterized by the non-linear dispersion scale σ_{NL}) in this work. The largest scale the survey can probe corresponds to a wave vector $k_{\text{min}} \simeq 2\pi/V_{\text{sur}}^{1/3}$ [90]. In our work, we choose the parameter set $\{p\}$ as $\{D_A(z), H(z), [f\sigma_8](z), [b_{\text{HI}}\sigma_8](z)\}$. Note that in Ref. [17] σ_{NL} is also treated as a free parameter, but in this work we ignore the small-scale non-linear FoG effect. When inverting the Fisher matrix, we can get the covariance matrix that gives us the forecasted constraint on the chosen parameter set. Note that we only use the forecasted cosmological observables $D_A(z)$, $H(z)$, and $[f\sigma_8](z)$ to constrain cosmological parameters.

B. Experimental configurations

In this paper, we focus on the Tianlai, BINGO, FAST, and SKA1-MID experiments. These experiments are potentially suitable for the HI IM survey in the post-reionization epoches of the universe. In this subsection, we give a brief description of these experiments.

Tianlai: The Tianlai project [91] is an HI IM experiment aimed at measuring the dark energy equation of state by detecting the BAO features in the large-scale structure power spectrum. The full-scale Tianlai cylinder array will consist of eight adjacent cylinders to be built in northwest China, with each cylinder 15 m wide and 120 m long with 256 dual polarization feeds [18, 44, 45]. Note that, currently, there is a Tianlai pathfinder array commissioning, which uses a much smaller scale cylinder array, but in this work we will only discuss the full-scale Tianlai cylinder array that is to be built in the future.

BINGO: The BINGO experiment [92] is a project to build a special-purpose radio telescope to map redshifted HI emission in the redshift range of $z = 0.13 - 0.48$. The design of BINGO is a dual-mirror compact antenna telescope with a 40 m primary mirror and an offset focus, which is proposed to have a receiver array containing 50–60 feed horns, with a 90 m focal length. It will be built in a disused open-caste gold mine in Uruguay [6, 32].

FAST: The FAST [93] is a multi-beam single dish telescope built in Guizhou province of southwest China. The aperture diameter is 500 m with an effective illuminating diameter of 300 m. It uses an active surface that adjusts shape to create parabolas in different directions. It will be capable of covering the sky within a 40-degree angle from the zenith. 19 beams are designed in one receiver array, which will greatly increase the survey speed [35, 36].

SKA1-MID: The SKA project [94], currently under construction, plans two stages of development. In this paper, we consider the SKA1-MID array, based in the Northern Cape, South Africa. SKA1-MID has 133 15 m SKA dishes and 64 13.5 m MeerKAT dishes. The SKA1-MID will perform an HI IM survey over a broad range of frequencies and a large fraction of the sky [24, 41, 42, 88]. Here we consider only the *Wide Band 1 Survey* of the SKA1-MID. In addition, in this work, for simplicity we consider SKA1-MID as an array with 197 15 m dishes.

The full instrumental parameters used for these experiments are listed in Table I.

C. Data and method

Method for forecasting cosmological constraints for HI IM surveys has been presented in Refs. [17, 95]. We will follow the prescription given in Refs. [17, 95] to perform the forecast for the 21 cm IM experiments. By performing measurements of the full anisotropic power spectrum, we obtain constraints on the angular diameter distance $D_A(z)$, the Hubble parameter $H(z)$, and the RSD observable $[f\sigma_8](z)$, which are considered to be indepen-

TABLE I. Experimental configurations for Tianlai, BINGO, FAST, and SKA1-MID.

	Tianlai	BINGO	FAST	SKA1-MID
z_{\min}	0	0.13	0	0.35
z_{\max}	2.55	0.48	0.35	3
N_{dish}	—	1	1	197
N_{beam}	1	50	19	1
D_{dish} [m]	—	40	300	15
S_{area} [deg ²]	10000	3000	20000	20000
t_{tot} [h]	10000	10000	10000	10000
T_{rec} [K]	50	50	20	Eq. (11)

dent in each redshift bin. We obtain covariance matrices for $\{D_A(z_j), H(z_j), [f\sigma_8](z_j); j = 1 \dots N\}$ in a series of N redshift bins $\{z_j\}$ by inverting the Fisher matrix. We perform the Fisher matrix calculations by considering the aforementioned parameters. The marginalized constraints on these parameters for these surveys are shown in Figure 1.

These covariance matrices, plus the fiducial cosmology, generate the mock data of these 21 cm IM experiments. Then we use these mock data to constrain cosmological parameters by performing a Markov Chain Monte Carlo (MCMC) analysis. In the MCMC analysis, we also employ the CMB data from the Planck 2018 release [85] and the BAO measurements from galaxy redshift surveys, including SDSS-MGS [96], 6dFGS [97], and BOSS DR12 [98].

In this paper, we employ the extended parametrized post-Friedmann (ePPF) framework to calculate the cosmological perturbations in the IDE scenario [66, 67]. This is because we need to avoid the perturbation divergence problem in the IDE cosmology.

It is well-known that, in the IDE scenario, when calculating the cosmological perturbations, it is found that for most cases the curvature perturbation on super-horizon scales at early times is divergent, which is a catastrophe for the IDE cosmology. The underlying reason of this problem is that we actually do not know how to consider the perturbations of dark energy. In the traditional linear perturbation theory, for calculating the perturbations of dark energy, we need to define a rest-frame sound speed for dark-energy fluid $c_s^2 = \delta p / \delta \rho$ (with the gauge $v|_{\text{rf}} = B|_{\text{rf}} = 0$) to relate the dark-energy density and pressure perturbations. This leads to that in a general gauge δp has two parts—adiabatic and nonadiabatic parts, and the interaction term appearing in the nonadiabatic part will occasionally leads the nonadiabatic modes to be unstable.

In order to solve this problem, Li, Zhang, and Zhang [66, 67] extended the original PPF framework [99] to include the IDE scenario, and used this method to avoid the divergence of cosmological perturbations in the IDE models. The PPF method does not consider the dark-energy pressure perturbation, but only describes dark-energy perturbations based on some basic facts of dark energy. On large scales, far beyond the horizon, the rela-

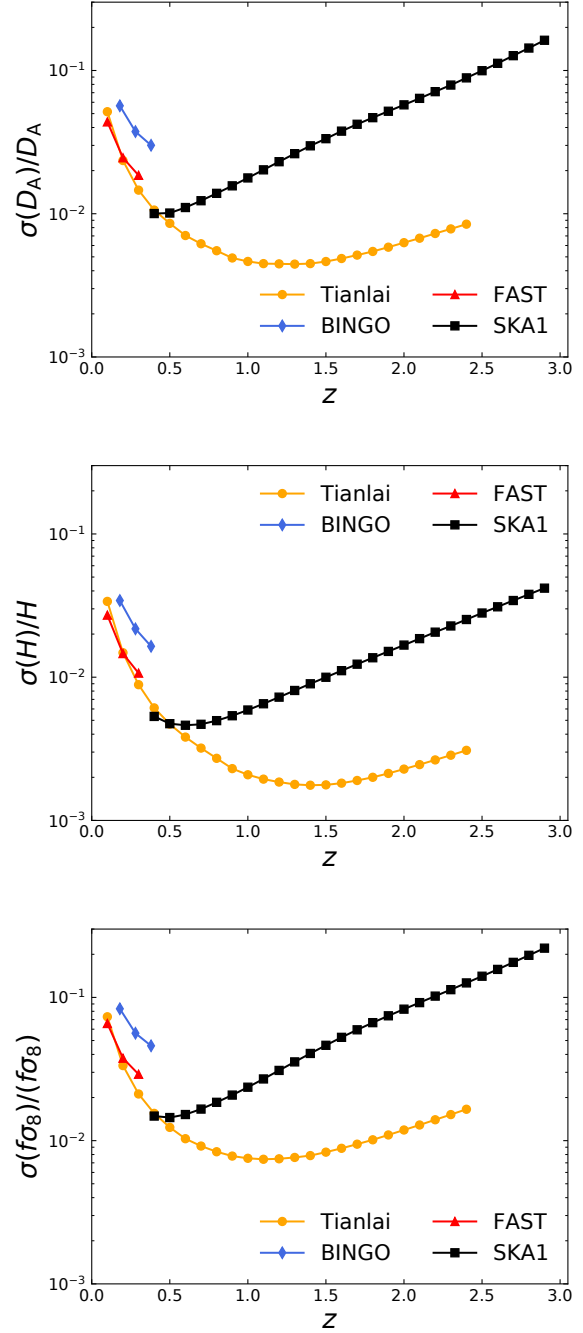


FIG. 1. Forecasted fractional errors on $D_A(z)$, $H(z)$, and $[f\sigma_8](z)$, as a function of redshift.

tionship between the velocities of dark energy and other components can be empirically parameterized. On small scales, deep inside the horizon, dark energy is smooth enough so that it can be viewed as a pure background. We thus can use the Poisson equation to describe this limit. In order to make these two limits compatible, we introduce a dynamical function Γ by which we can find an equation to describe the cases on all scales. In the

TABLE II. The 1σ errors on the parameters in the Λ CDM model from the different data combinations.

	β	H_0 [km s $^{-1}$ Mpc $^{-1}$]	Ω_m	σ_8
Planck	0.00240	1.80	0.0256	0.0150
Planck+BAO	0.00120	0.69	0.0087	0.0110
Tianlai	0.00196	0.10	0.0013	0.0015
Planck+Tianlai	0.00052	0.09	0.0011	0.0011
Planck+BINGO	0.00150	0.98	0.0130	0.0110
Planck+FAST	0.00110	0.65	0.0086	0.0088
Planck+SKA1-MID	0.00057	0.22	0.0029	0.0023

TABLE III. The 1σ errors on the parameters in the Iw CDM model from the different data combinations.

	β	w
Planck	0.00176	0.324
Planck+BAO	0.00150	0.074
Tianlai	0.00742	0.010
Planck+Tianlai	0.00058	0.006
Planck+BINGO	0.00140	0.038
Planck+FAST	0.00130	0.030
Planck+SKA1-MID	0.00079	0.010

equation of motion of Γ , a parameter c_T is introduced, giving a transition scale in terms of the Hubble scale under which dark energy is smooth enough. In this equation, there is no perturbation variable of dark energy, and when the evolution of Γ is derived, we can directly obtain the density perturbation and velocity perturbation of dark energy. Hence, this method avoids using the pressure perturbation of dark energy defined by the sound speed. Here, we only give a very brief description of the ePPF method, and we refer the reader to Refs. [66, 67] for more details.

We employ the CosmoMC package [100] to perform the MCMC calculations and insert the ePPF code as a part of it to treat the cosmological perturbations in the IDE models.

III. RESULTS

In this section, we will present the forecasted results showing relative constraining capabilities for the Λ CDM and Iw CDM models by combining each of the 21 cm IM experiments with Planck. Tables II and III list the 1σ errors for the marginalized parameter constraints for the Λ CDM and Iw CDM models, respectively. In Section III A, we will show what role the 21 cm IM experiments, taking the example of Tianlai, could play in constraining cosmological parameters, and compare with the BAO measurements from galaxy redshift surveys. In Section III B, we will compare the capabilities of constraining cosmological parameters for the different 21 cm IM experiments.

A. Constraints on cosmological parameters from the Tianlai cylinder array

The 1σ and 2σ posterior distribution contours are shown in Figure 2 for Planck, Planck+BAO, Tianlai, and Planck+Tianlai in the Λ CDM model. We find that the future full-scale Tianlai experiment can give very tight constraints on H_0 , Ω_m and σ_8 . With the Tianlai data alone, we obtain $\sigma(H_0) = 0.10$ km s $^{-1}$ Mpc $^{-1}$, $\sigma(\Omega_m) = 0.0013$, and $\sigma(\sigma_8) = 0.0015$, which are even much better than the results of $\sigma(H_0) = 0.69$ km s $^{-1}$ Mpc $^{-1}$, $\sigma(\Omega_m) = 0.0087$, and $\sigma(\sigma_8) = 0.0110$ from Planck+optical BAO. Comparing with the Planck data, the data combination of Planck+Tianlai can improve the constraint accuracies of H_0 , Ω_m and σ_8 by $(1.80 - 0.09)/1.80 = 95.0\%$, $(0.0256 - 0.0011)/0.0256 = 95.7\%$ and $(0.0150 - 0.0011)/0.0150 = 92.7\%$, respectively.

The Tianlai experiment can also give a moderate constraint on the coupling parameter β with $\sigma(\beta) \approx 0.002$, which is similar to the Planck-alone result, and actually slightly better. In fact, for the IDE model with $Q = \beta H \rho_c$, the CMB data usually could provide a tight constraint on the coupling parameter β . This is because in the early universe both H and ρ_c take rather high values, and the energy transfer rate Q can take a moderate value even if β is very small. Thus, the CMB data as an early-universe probe can give a relatively tight constraint on β . This is why the Planck CMB data can offer a similar constraint on β , compared with the case of the Tianlai data, but for the other cosmological parameters the Tianlai data can give much better constraints. Since the degeneracy directions of β and other parameters for Planck and Tianlai are rather different, we can eventually obtain a rather tight constraint on β , i.e., $\sigma(\beta) = 0.00052$, from the Planck+Tianlai data combination, which is much better than the result of $\sigma(\beta) = 0.00120$ from the Planck+BAO data combination.

In Figure 3, we show the constraint results of the Iw CDM model. Here we only show the posterior distribution contours in the β - w plane that we are most interested in. We can see that using only the Planck CMB data cannot give a good constraint on dark energy EoS parameter w , i.e., $\sigma(w) \approx 0.3$. It is necessary to use the late-universe measurements to break the parameter degeneracies inherent in CMB. As a contrast, the Tianlai-alone data can provide a rather tight constraint on w , giving the result of $\sigma(w) = 0.01$.

However, as discussed above, the CMB data can tightly constrain the coupling parameter β in the Iw CDM model with the interaction term $Q = \beta H \rho_c$. So, we can see that the Planck-alone data give $\sigma(\beta) = 0.00176$, which is much better than the result given by the Tianlai-alone data, $\sigma(\beta) = 0.00742$.

Since the CMB data can tightly constrain β and the Tianlai data can tightly constrain w , the degeneracy directions of them are entirely different. It is known that

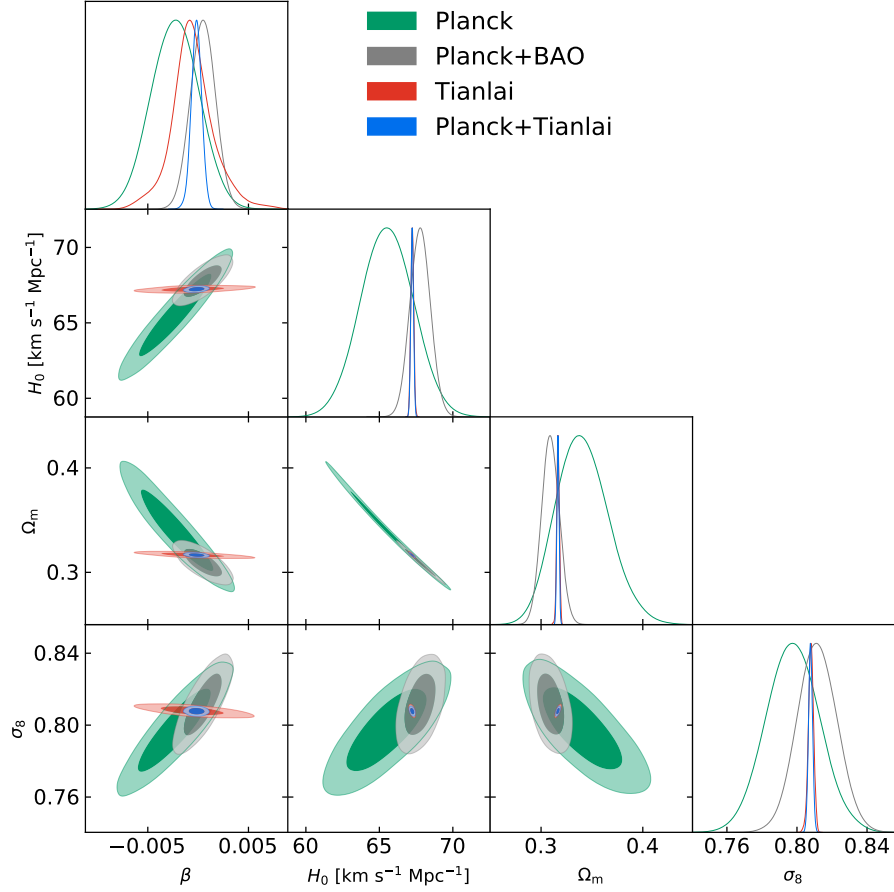


FIG. 2. Constraints on cosmological parameters from Planck, Planck+BAO, Tianlai, and Planck+Tianlai in the Λ CDM model.

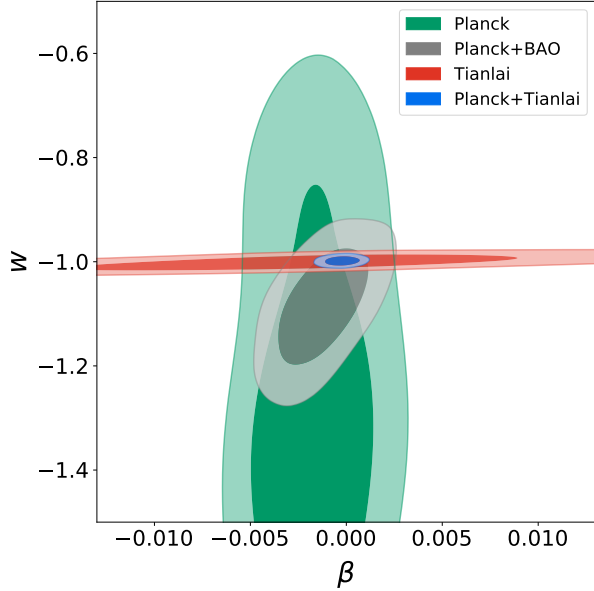


FIG. 3. Constraints on β and w from Planck, Planck+BAO, Tianlai, and Planck+Tianlai in the Iw CDM model.

Planck-alone, and even Planck+BAO, can only provide a loose or a moderate constraint on the Iw CDM model, as shown in Figure 3. Nevertheless, since the cosmological parameter degeneracies can be broken by the Tianlai data, the parameter constraints are greatly improved by adding the Tianlai data in the fit. We obtain $\sigma(\beta) = 0.00058$ and $\sigma(w) = 0.006$ from the Planck+Tianlai data combination, and we find that the constraints on β and w are improved by $(0.00176 - 0.00058)/0.00176 = 67.0\%$ and $(0.324 - 0.006)/0.324 = 98.1\%$, respectively, by adding the Tianlai data. Comparing with the constraint results of $\sigma(\beta) = 0.00150$ and $\sigma(w) = 0.074$ from Planck+BAO, we can see that the future 21 IM experiments will exhibit powerful capability of constraining cosmological parameters.

B. Comparison with constraints from different 21 cm IM experiments

In this subsection, we will discuss the ability to constrain cosmological parameters for the different 21 cm IM experiments.

Figure 4 visualizes the constraint results for the Λ CDM model from each of these experiments, includ-

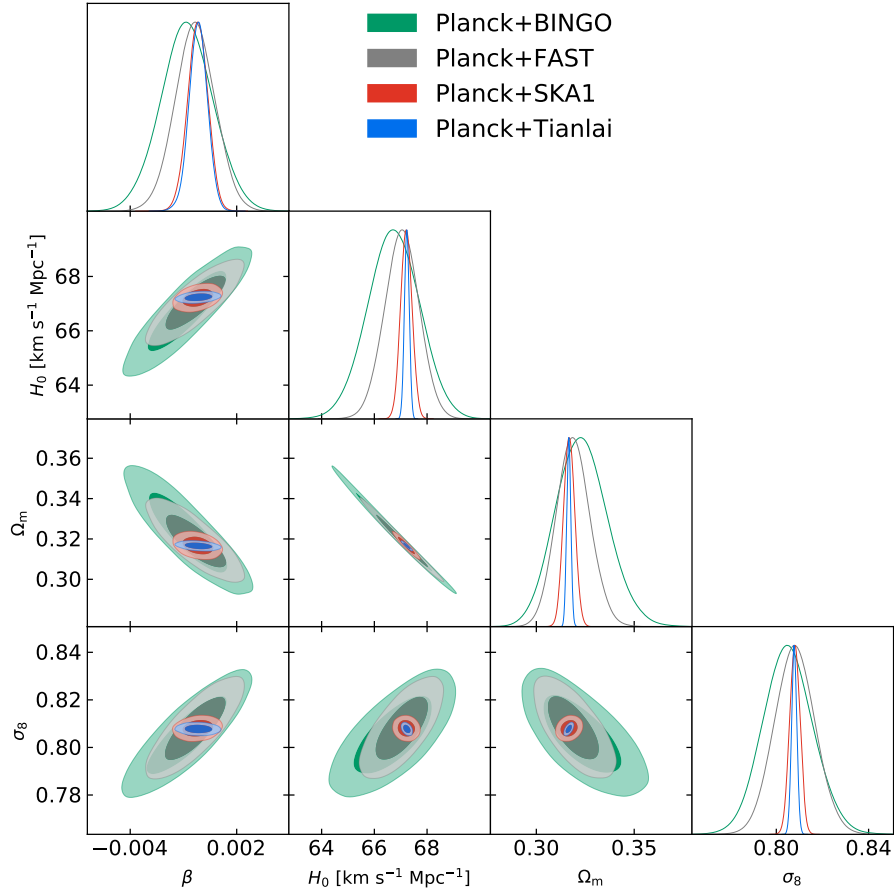


FIG. 4. Constraints on cosmological parameters from Planck+BINGO, Planck+FAST, Planck+SKA1-MID, and Planck+Tianlai in the Λ CDM model.

ing BINGO, FAST, SKA1-MID, and Tianlai, combined with Planck. We can clearly see from Figure 4 that the constraining capabilities of the two arrays, i.e. Tianlai and SKA1-MID, are much better than those of the single dishes, FAST and BINGO. Comparing Tianlai and SKA1-MID, Tianlai is evidently better, and comparing FAST and BINGO, FAST is much better. As shown in Figure 1, FAST and BINGO can only observe in low redshifts and can only cover narrow redshift ranges, i.e., $0 < z < 0.35$ for FAST and $0.13 < z < 0.48$ for BINGO. Although the redshift range coverages are similar, comparing FAST and BINGO for the relative measurement errors on $D_A(z)$, $H(z)$ and $[f\sigma_8](z)$, we find that obviously FAST is better than BINGO, mainly due to the much larger survey area and the larger aperture size. Comparing Tianlai and SKA1-MID, we find that both of them can cover a wide redshift range, i.e., $0 < z < 2.55$ for Tianlai and $0.35 < z < 3$ for SKA1-MID (Wide Band 1 Survey). However, for the redshift range of $z > 0.5$, the relative errors on $D_A(z)$, $H(z)$, and $[f\sigma_8](z)$ of Tianlai are much smaller than those of SKA1-MID. This highlights the advantage of a compact interferometer array with a large number of receivers, and explains why the Tianlai's capability of constraining cosmological param-

eters is better than SKA1-MID.

Concretely, for constraining the coupling parameter β , we obtain $\sigma(\beta) = 0.00150, 0.00110, 0.00057$, and 0.00052 , from Planck+BINGO, Planck+FAST, Planck+SKA1-MID, and Planck+Tianlai, respectively. This shows that, for constraining β in the Λ CDM model, the capabilities of SKA1-MID and Tianlai are similar, although Tianlai is slightly better, in the sense of combining with Planck, both are much better than those of BINGO and FAST. Comparing with the results of the Planck-alone data, the Planck+BINGO, Planck+FAST, Planck+SKA1-MID, and Planck+Tianlai data can improve the constraints on β by 37.5%, 54.2%, 76.3%, and 78.3%, respectively.

We then show the results for the constraints on the other cosmological parameters in the Λ CDM model. We obtain $\sigma(H_0) = 0.98 \text{ km s}^{-1} \text{ Mpc}^{-1}$, $\sigma(\Omega_m) = 0.0130$, and $\sigma(\sigma_8) = 0.0110$ from Planck+BINGO, and $\sigma(H_0) = 0.65 \text{ km s}^{-1} \text{ Mpc}^{-1}$, $\sigma(\Omega_m) = 0.0086$, and $\sigma(\sigma_8) = 0.0088$ from Planck+FAST. We can see that, for constraining H_0 , Ω_m , and σ_8 , FAST performs much better than BINGO. But we also notice that neither FAST nor BINGO is as powerful as Tianlai and SKA1-MID. We obtain $\sigma(H_0) = 0.22 \text{ km s}^{-1} \text{ Mpc}^{-1}$, $\sigma(\Omega_m) =$

0.0029, and $\sigma(\sigma_8) = 0.0023$ from Planck+SKA1-MID, and $\sigma(H_0) = 0.09 \text{ km s}^{-1} \text{ Mpc}^{-1}$, $\sigma(\Omega_m) = 0.0011$, and $\sigma(\sigma_8) = 0.0011$ from Planck+Tianlai. We can clearly see that in the future the full-scale Tianlai cylinder array experiment will play a significant role in precisely measuring cosmological parameters.

Here we note that, in this work, we only discuss the Wide Band 1 Survey of the SKA1-MID. Actually, SKA1 has another two surveys targeting cosmology, i.e., Medium-Deep Band 2 Survey (with SKA1-MID) and Deep SKA-LOW Survey (with SKA1-LOW). The Medium-Deep Band 2 Survey covers the redshift range of $0 < z < 0.5$ (with $S_{\text{area}} = 5000 \text{ deg}^2$ and $t_{\text{total}} = 10000 \text{ h}$), and Deep SKA-LOW Survey covers the redshift range of $3 < z < 6$ (with $S_{\text{area}} = 100 \text{ deg}^2$ and $t_{\text{total}} = 5000 \text{ h}$). It is of great interest to use the combination of the three surveys of SKA1 in measuring the expansion history of the post-reionization epoch of the universe to explore various cosmological issues. We will leave this work in the future.

In order to compare their constraint abilities in the $Iw\text{CDM}$ model, we show the 1σ and 2σ measurement error contours for Planck+BINGO, Planck+FAST, Planck+SKA1-MID and Planck+Tianlai in Figure 5. We obtain $\sigma(\beta) = 0.00140$ and $\sigma(w) = 0.038$ from Planck+BINGO, which are improved by 20.5% and 88.3%, respectively, when combining the BINGO data in the cosmological fit to the Planck CMB data. This shows that, although BINGO's constraining capability is the weakest among the four 21 cm IM experiments considered in this work, it still can play an important role in breaking the parameter degeneracies in CMB and in improving the measurement accuracies of cosmological parameters (both β and w) in the $Iw\text{CDM}$ model. FAST performs slightly better than BINGO, and we obtain $\sigma(\beta) = 0.00130$ and $\sigma(w) = 0.030$ from Planck+FAST. Evidently, SKA1-MID performs much better than BINGO and FAST, and we obtain $\sigma(\beta) = 0.00079$ and $\sigma(w) = 0.010$ from Planck+SKA1-MID. The most stringent constraints on the $Iw\text{CDM}$ model are from Planck+Tianlai, and in this case we have $\sigma(\beta) = 0.00058$ and $\sigma(w) = 0.006$. Compared with the Planck result, we find that FAST, SKA1-MID, and Tianlai can improve the constraints on β by 26.1%, 55.1%, and 67.0%, respectively.

IV. CONCLUSION

In this work, we investigate the constraint capabilities of the future 21 cm IM experiments for the interacting dark energy model. We consider BINGO, FAST, SKA1-MID, and Tianlai as typical examples of 21 cm IM experiments, and find that among them a compact interferometer array like the full-scale Tianlai cylinder array would be the best one in constraining the interacting dark energy model.

We find that the 21 cm observations with the full-scale

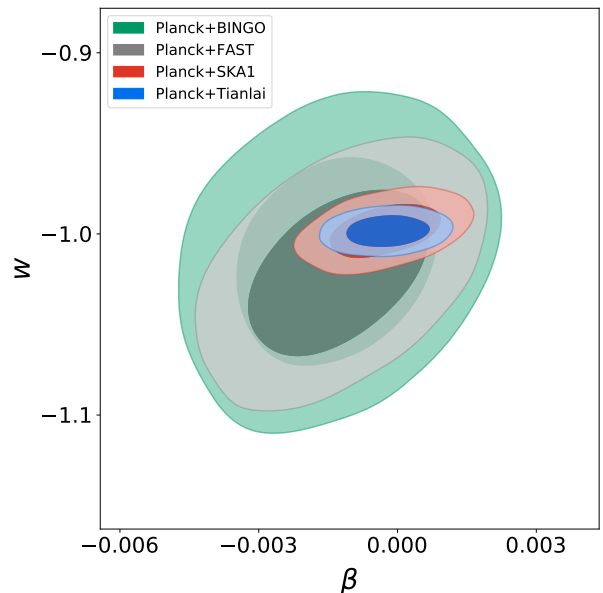


FIG. 5. Constraints on β and w from Planck+BINGO, Planck+FAST, Planck+SKA1-MID, and Planck+Tianlai in the $Iw\text{CDM}$ model.

Tianlai cylinder array can tightly constrain H_0 , Ω_m , and σ_8 . For example, in the ΛCDM model, the Tianlai-alone data can give the constraint accuracies of $\sigma(H_0) = 0.10 \text{ km s}^{-1} \text{ Mpc}^{-1}$, $\sigma(\Omega_m) = 0.0013$, and $\sigma(\sigma_8) = 0.0015$, even much better than those of Planck+optical BAO. But, relatively speaking, the Tianlai data cannot provide a tight constraint on the coupling parameter β as much as constraints on other cosmological parameters. However, it is also found that the parameter degeneracy directions from Planck and Tianlai are entirely different, and thus the combination of Planck and Tianlai can well break the parameter degeneracies and give a rather tight constraint on β . In the ΛCDM and $Iw\text{CDM}$ models, we obtain $\sigma(\beta) = 5.2 \times 10^{-4}$ and 5.8×10^{-4} , respectively, from Planck+Tianlai. This shows that the constraints on β can be improved by 78.3% and 67.0% in the two models by adding the Tianlai data in the cosmological fit, compared with the case of using only the Planck data.

We also make a detailed comparison for BINGO, FAST, SKA1-MID, and Tianlai in the cosmological-fit study of the interacting dark energy model. We find that, for the constraint capability, Tianlai is the best one, and SKA1-MID is slightly less powerful than Tianlai, but both are much better than FAST and BINGO. Our goal is not to show the superiority or inferiority of these experiments against each other, but to give a global picture on their relative prospects. Our results show that the 21 cm IM experiments will provide a promising tool for exploring the nature of dark energy, and in particular a compact interferometer array will play a significant role in measuring the coupling between dark energy and dark matter.

ACKNOWLEDGMENTS

We would like to thank Xin Wang, Xuelei Chen, Ling-Feng Wang, Li-Yang Gao, Peng-Ju Wu, and Yue Shao for helpful discussions. This work was supported by the MoST-BRICS Flagship Project No. 2018YFE0120800, the National Natural Science Foundation of China (Grant Nos. 11975072, 11875102, 11835009, 11690021,

11973047, and 11633004), National SKA Program of China No. 2020SKA0110401, the Chinese Academy of Sciences (CAS) Strategic Priority Research Program XDA15020200, the Liaoning Revitalization Talents Program (Grant No. XLYC1905011), the Fundamental Research Funds for the Central Universities (Grant No. N2005030), and the Top-Notch Young Talents Program of China (Grant No. W02070050).

-
- [1] Adam G. Riess et al. Observational evidence from supernovae for an accelerating universe and a cosmological constant. *Astron. J.*, 116:1009–1038, 1998.
 - [2] Chris Blake and Karl Glazebrook. Probing dark energy using baryonic oscillations in the galaxy power spectrum as a cosmological ruler. *Astrophys. J.*, 594:665–673, 2003.
 - [3] Hee-Jong Seo and Daniel J. Eisenstein. Probing dark energy with baryonic acoustic oscillations from future large galaxy redshift surveys. *Astrophys. J.*, 598:720–740, 2003.
 - [4] Tzu-Ching Chang, Ue-Li Pen, Jeffrey B. Peterson, and Patrick McDonald. Baryon Acoustic Oscillation Intensity Mapping as a Test of Dark Energy. *Phys. Rev. Lett.*, 100:091303, 2008.
 - [5] Richard A. Battye, Rod D. Davies, and Jochen Weller. Neutral hydrogen surveys for high redshift galaxy clusters and proto-clusters. *Mon. Not. Roy. Astron. Soc.*, 355:1339–1347, 2004.
 - [6] R.A. Battye, I.W.A. Browne, C. Dickinson, G. Heron, B. Maffei, and A. Pourtsidou. HI intensity mapping : a single dish approach. *Mon. Not. Roy. Astron. Soc.*, 434:1239–1256, 2013.
 - [7] Matthew McQuinn, Oliver Zahn, Matias Zaldarriaga, Lars Hernquist, and Steven R. Furlanetto. Cosmological parameter estimation using 21 cm radiation from the epoch of reionization. *Astrophys. J.*, 653:815–830, 2006.
 - [8] Abraham Loeb and Stuart Wyithe. Precise Measurement of the Cosmological Power Spectrum With a Dedicated 21cm Survey After Reionization. *Phys. Rev. Lett.*, 100:161301, 2008.
 - [9] Jonathan R. Pritchard and Abraham Loeb. Evolution of the 21 cm signal throughout cosmic history. *Phys. Rev. D*, 78:103511, 2008.
 - [10] Stuart Wyithe and Abraham Loeb. Fluctuations in 21cm Emission After Reionization. *Mon. Not. Roy. Astron. Soc.*, 383:606, 2008.
 - [11] Yi Mao, Max Tegmark, Matthew McQuinn, Matias Zaldarriaga, and Oliver Zahn. How accurately can 21 cm tomography constrain cosmology? *Phys. Rev. D*, 78:023529, 2008.
 - [12] Stuart Wyithe, Abraham Loeb, and Paul Geil. Baryonic Acoustic Oscillations in 21cm Emission: A Probe of Dark Energy out to High Redshifts. *Mon. Not. Roy. Astron. Soc.*, 383:1195, 2008.
 - [13] J.S. Bagla, Nishikanta Khandai, and Kanan K. Datta. HI as a Probe of the Large Scale Structure in the Post-Reionization Universe. *Mon. Not. Roy. Astron. Soc.*, 407:567, 2010.
 - [14] Hee-Jong Seo, Scott Dodelson, John Marriner, Dave McGinnis, Albert Stebbins, Chris Stoughton, and Alberto Vallinotto. A ground-based 21cm Baryon acoustic oscillation survey. *Astrophys. J.*, 721:164–173, 2010.
 - [15] Adam Lidz, Steven R. Furlanetto, S.Peng Oh, James Aguirre, Tzu-Ching Chang, Olivier Dore, and Jonathan R. Pritchard. Intensity Mapping with Carbon Monoxide Emission Lines and the Redshifted 21 cm Line. *Astrophys. J.*, 741:70, 2011.
 - [16] R. Ansari, J.E. Campagne, P. Colom, J.M.Le Goff, C. Magneville, J.M. Martin, M. Moniez, J. Rich, and C. Yeche. 21 cm observation of LSS at $z \sim 1$ Instrument sensitivity and foreground subtraction. *Astron. Astrophys.*, 540:A129, 2012.
 - [17] Philip Bull, Pedro G. Ferreira, Prina Patel, and Mario G. Santos. Late-time cosmology with 21cm intensity mapping experiments. *Astrophys. J.*, 803(1):21, 2015.
 - [18] Yidong Xu, Xin Wang, and Xuelei Chen. Forecasts on the Dark Energy and Primordial Non-Gaussianity Observations with the Tianlai Cylinder Array. *Astrophys. J.*, 798(1):40, 2015.
 - [19] Alkistis Pourtsidou, David Bacon, and Robert Crittenden. HI and cosmological constraints from intensity mapping, optical and CMB surveys. *Mon. Not. Roy. Astron. Soc.*, 470(4):4251–4260, 2017.
 - [20] Elimboto Yohana, Yi-Chao Li, and Yin-Zhe Ma. Forecasts of cosmological constraints from HI intensity mapping with FAST, BINGO & SKA-I. 8 2019.
 - [21] Denis Tramonte and Yin-Zhe Ma. The neutral hydrogen distribution in large-scale haloes from 21-cm intensity maps. *Mon. Not. Roy. Astron. Soc.*, 498(4):5916–5935, 2020.
 - [22] Phil Bull, Stefano Camera, Alvise Raccanelli, Chris Blake, Pedro Ferreira, Mario Santos, and Dominik J. Schwarz. Measuring baryon acoustic oscillations with future SKA surveys. *PoS, AASKA14:024*, 2015.
 - [23] Philip Bull. Extending cosmological tests of General Relativity with the Square Kilometre Array. *Astrophys. J.*, 817(1):26, 2016.
 - [24] Robert Braun, Tyler Bourke, James A Green, Evan Keane, and Jeff Wagg. Advancing Astrophysics with the Square Kilometre Array. *PoS, AASKA14:174*, 2015.
 - [25] YiDong Xu and Xin Zhang. Cosmological parameter measurement and neutral hydrogen 21 cm sky survey with the Square Kilometre Array. *Sci. China Phys. Mech. Astron.*, 63(7):270431, 2020.
 - [26] Jing-Fei Zhang, Li-Yang Gao, Dong-Ze He, and Xin Zhang. Improving cosmological parameter estimation with the future 21 cm observation from SKA. *Phys. Lett. B*, 799:135064, 2019.
 - [27] Jing-Fei Zhang, Bo Wang, and Xin Zhang. Forecast for weighing neutrinos in cosmology with SKA. *Sci. China*

- Phys. Mech. Astron.*, 63(8):280411, 2020.
- [28] Denis Tramonete, Yin-Zhe Ma, Yi-Chao Li, and Lister Staveley-Smith. Searching for H I imprints in cosmic web filaments with 21-cm intensity mapping. *Mon. Not. Roy. Astron. Soc.*, 489(1):385–400, 2019.
 - [29] Tzu-Ching Chang, Ue-Li Pen, Kevin Bandura, and Jeffrey B. Peterson. Hydrogen 21-cm Intensity Mapping at redshift 0.8. *Nature*, 466:463–465, 2010.
 - [30] K.W. Masui et al. Measurement of 21 cm brightness fluctuations at $z \sim 0.8$ in cross-correlation. *Astrophys. J. Lett.*, 763:L20, 2013.
 - [31] C.J. Anderson et al. Low-amplitude clustering in low-redshift 21-cm intensity maps cross-correlated with 2dF galaxy densities. *Mon. Not. Roy. Astron. Soc.*, 476(3):3382–3392, 2018.
 - [32] Clive Dickinson. BINGO - A novel method to detect BAOs using a total-power radio telescope. In *49th Rencontres de Moriond on Cosmology*, pages 139–142, 2014.
 - [33] C.A. Wuensche. The BINGO telescope: a new instrument exploring the new 21 cm cosmology window. *J. Phys. Conf. Ser.*, 1269(1):012002, 2019.
 - [34] C.A. Wuensche et al. Baryon acoustic oscillations from Integrated Neutral Gas Observations: Broadband corrugated horn construction and testing. *Exper. Astron.*, 50(1):125–144, 2020.
 - [35] Rendong Nan, Di Li, Chengjin Jin, Qiming Wang, Lichun Zhu, Wenbai Zhu, Haiyan Zhang, Youling Yue, and Lei Qian. The Five-Hundred-Meter Aperture Spherical Radio Telescope (FAST) Project. *Int. J. Mod. Phys. D*, 20:989–1024, 2011.
 - [36] George F. Smoot and Ivan Debono. 21 cm intensity mapping with the Five hundred metre Aperture Spherical Telescope. *Astron. Astrophys.*, 597:A136, 2017.
 - [37] Marie-Anne Bigot-Sazy, Yin-Zhe Ma, Richard A. Battye, Ian W. A. Browne, Tianyue Chen, Clive Dickinson, Stuart Harper, Bruno Maffei, Lucas C. Olivari, and Peter N. Wilkinson. HI intensity mapping with FAST. *ASP Conf. Ser.*, 502:41, 2016.
 - [38] Di Li, Rendong Nan, and Zhichen Pan. The Five-hundred-meter Aperture Spherical radio Telescope project and its early science opportunities. *IAU Symp.*, 291:325–330, 2013.
 - [39] Hao-Ran Yu, Ue-Li Pen, Tong-Jie Zhang, Di Li, and Xuelei Chen. Blind search for 21-cm absorption systems using a new generation of Chinese radio telescopes. *Res. Astron. Astrophys.*, 17(6):049, 2017.
 - [40] Wenkai Hu, Xin Wang, Fengquan Wu, Yougang Wang, Pengjie Zhang, and Xuelei Chen. Forecast for FAST: from Galaxies Survey to Intensity Mapping. *Mon. Not. Roy. Astron. Soc.*, 493(4):5854–5870, 2020.
 - [41] Philip Bull, Stefano Camera, Alvise Raccanelli, Chris Blake, Pedro G. Ferreira, Mario G. Santos, and Dominik J. Schwarz. Measuring baryon acoustic oscillations with future SKA surveys. 1 2015.
 - [42] Mario G. Santos et al. Cosmology from a SKA HI intensity mapping survey. *PoS, AASKA14*:019, 2015.
 - [43] Robert Braun, Anna Bonaldi, Tyler Bourke, Evan Keane, and Jeff Wagg. Anticipated Performance of the Square Kilometre Array – Phase 1 (SKA1). 12 2019.
 - [44] Xuelei Chen. Radio detection of dark energy—the Tianlai project. *Scientia Sinica Physica, Mechanica & Astronomica*, 41(12):1358, January 2011.
 - [45] Xuelei Chen. The Tianlai Project: a 21CM Cosmology Experiment. In *International Journal of Modern Physics Conference Series*, volume 12 of *International Journal of Modern Physics Conference Series*, pages 256–263, March 2012.
 - [46] Fengquan Wu, Yougang Wang, Juyong Zhang, Huli Shi, and Xuelei Chen. Tianlai: a 21cm radio telescope array for BAO and dark energy, status and progress. In *51st Rencontres de Moriond on Cosmology*, pages 315–318. ARISF, 2016.
 - [47] JiXia Li, ShiFan Zuo, FengQuan Wu, YouGang Wang, JuYong Zhang, ShiJie Sun, YiDong Xu, ZiJie Yu, Reza Ansari, YiChao Li, Albert Stebbins, Peter Timbie, YanPing Cong, JingChao Geng, Jie Hao, QiZhi Huang, JianBin Li, Rui Li, DongHao Liu, YingFeng Liu, Tao Liu, John P. Marriner, ChenHui Niu, Ue-Li Pen, Jeffery B. Peterson, HuLi Shi, Lin Shu, YaFang Song, Hai-Jun Tian, GuiSong Wang, QunXiong Wang, RongLi Wang, WeiXia Wang, Xin Wang, KaiFeng Yu, Jiao Zhang, BoQin Zhu, JiaLu Zhu, and XueLei Chen. The Tianlai Cylinder Pathfinder array: System functions and basic performance analysis. *Science China Physics, Mechanics, and Astronomy*, 63(12):129862, September 2020.
 - [48] Fengquan Wu, Jixia Li, Shifan Zuo, Xuelei Chen, Santanu Das, John P. Marriner, Trevor M. Oxholm, Anh Phan, Albert Stebbins, Peter T. Timbie, Reza Ansari, Jean-Eric Campagne, Zhiping Chen, Yanping Cong, Qizhi Huang, Yichao Li, Tao Liu, Yingfeng Liu, Chenhui Niu, Calvin Osinga, Olivier Perdureau, Jeffrey B. Peterson, Huli Shi, Gage Siebert, Shijie Sun, Haijun Tian, Gregory S. Tucker, Qunxiong Wang, Rongli Wang, Yougang Wang, Yanlin Wu, Yidong Xu, Kaifeng Yu, Zijie Yu, Jiao Zhang, Juyong Zhang, and Jialu Zhu. The Tianlai Dish Pathfinder Array: design, operation and performance of a prototype transit radio interferometer. *arXiv e-prints*, page arXiv:2011.05946, November 2020.
 - [49] B. Wang, E. Abdalla, F. Atrio-Barandela, and D. Pavon. Dark Matter and Dark Energy Interactions: Theoretical Challenges, Cosmological Implications and Observational Signatures. *Rept. Prog. Phys.*, 79(9):096901, 2016.
 - [50] Luca Amendola. Coupled quintessence. *Phys. Rev. D*, 62:043511, 2000.
 - [51] Xin Zhang. Coupled quintessence in a power-law case and the cosmic coincidence problem. *Mod. Phys. Lett. A*, 20:2575, 2005.
 - [52] Xin Zhang. Statefinder diagnostic for coupled quintessence. *Phys. Lett. B*, 611:1–7, 2005.
 - [53] Xin Zhang, Feng-Quan Wu, and Jingfei Zhang. A New generalized Chaplygin gas as a scheme for unification of dark energy and dark matter. *JCAP*, 01:003, 2006.
 - [54] John D. Barrow and T. Clifton. Cosmologies with energy exchange. *Phys. Rev. D*, 73:103520, 2006.
 - [55] Jingfei Zhang, Hongya Liu, and Xin Zhang. Statefinder diagnosis for the interacting model of holographic dark energy. *Phys. Lett. B*, 659:26–33, 2008.
 - [56] Jian-Hua He and Bin Wang. Effects of the interaction between dark energy and dark matter on cosmological parameters. *JCAP*, 06:010, 2008.
 - [57] Jian-Hua He, Bin Wang, and Y.P. Jing. Effects of dark sectors’ mutual interaction on the growth of structures. *JCAP*, 07:030, 2009.
 - [58] Jussi Valiviita, Roy Maartens, and Elisabetta Majerotto. Observational constraints on an interacting

- dark energy model. *Mon. Not. Roy. Astron. Soc.*, 402:2355–2368, 2010.
- [59] Christian G. Boehmer, Gabriela Caldera-Cabral, Ruth Lazkoz, and Roy Maartens. Dynamics of dark energy with a coupling to dark matter. *Phys. Rev. D*, 78:023505, 2008.
- [60] Jik-Su Kim, Chol-Jun Kim, Sin Chol Hwang, and Yong Hae Ko. Scalar - Tensor gravity with scalar - matter direct coupling and its cosmological probe. *Phys. Rev. D*, 96(4):043507, 2017.
- [61] Jun-Qing Xia. Constraint on coupled dark energy models from observations. *Phys. Rev. D*, 80:103514, 2009.
- [62] Hao Wei. Cosmological Constraints on the Sign-Changeable Interactions. *Commun. Theor. Phys.*, 56:972–980, 2011.
- [63] Yun-He Li and Xin Zhang. Running coupling: Does the coupling between dark energy and dark matter change sign during the cosmological evolution? *Eur. Phys. J. C*, 71:1700, 2011.
- [64] Timothy Clemson, Kazuya Koyama, Gong-Bo Zhao, Roy Maartens, and Jussi Valiviita. Interacting Dark Energy – constraints and degeneracies. *Phys. Rev. D*, 85:043007, 2012.
- [65] Yun-He Li and Xin Zhang. Large-scale stable interacting dark energy model: Cosmological perturbations and observational constraints. *Phys. Rev. D*, 89(8):083009, 2014.
- [66] Yun-He Li, Jing-Fei Zhang, and Xin Zhang. Parametrized Post-Friedmann Framework for Interacting Dark Energy. *Phys. Rev. D*, 90(6):063005, 2014.
- [67] Yun-He Li, Jing-Fei Zhang, and Xin Zhang. Exploring the full parameter space for an interacting dark energy model with recent observations including redshift-space distortions: Application of the parametrized post-Friedmann approach. *Phys. Rev. D*, 90(12):123007, 2014.
- [68] Xin Zhang. Probing the interaction between dark energy and dark matter with the parametrized post-Friedmann approach. *Sci. China Phys. Mech. Astron.*, 60(5):050431, 2017.
- [69] Jing-Lei Cui, Lu Yin, Ling-Feng Wang, Yun-He Li, and Xin Zhang. A closer look at interacting dark energy with statefinder hierarchy and growth rate of structure. *JCAP*, 09:024, 2015.
- [70] Shuang Wang, Yong-Zhen Wang, Jia-Jia Geng, and Xin Zhang. Effects of time-varying β in SNLS3 on constraining interacting dark energy models. *Eur. Phys. J. C*, 74(11):3148, 2014.
- [71] Jia-Jia Geng, Yun-He Li, Jing-Fei Zhang, and Xin Zhang. Redshift drift exploration for interacting dark energy. *Eur. Phys. J. C*, 75(8):356, 2015.
- [72] Jussi Väliiviita and Elina Palmgren. Distinguishing interacting dark energy from Λ CDM with CMB, lensing, and baryon acoustic oscillation data. *JCAP*, 07:015, 2015.
- [73] Eleonora Di Valentino, Alessandro Melchiorri, Olga Mena, and Sunny Vagnozzi. Nonminimal dark sector physics and cosmological tensions. *Phys. Rev. D*, 101(6):063502, 2020.
- [74] Rui-Yun Guo, Yun-He Li, Jing-Fei Zhang, and Xin Zhang. Weighing neutrinos in the scenario of vacuum energy interacting with cold dark matter: application of the parameterized post-Friedmann approach. *JCAP*, 05:040, 2017.
- [75] Rui-Yun Guo, Jing-Fei Zhang, and Xin Zhang. Exploring neutrino mass and mass hierarchy in the scenario of vacuum energy interacting with cold dark matter. *Chin. Phys. C*, 42(9):095103, 2018.
- [76] Rui-Yun Guo, Jing-Fei Zhang, and Xin Zhang. Can the H_0 tension be resolved in extensions to Λ CDM cosmology? *JCAP*, 02:054, 2019.
- [77] Weiqiang Yang, Supriya Pan, Eleonora Di Valentino, Rafael C. Nunes, Sunny Vagnozzi, and David F. Mota. Tale of stable interacting dark energy, observational signatures, and the H_0 tension. *JCAP*, 09:019, 2018.
- [78] Lu Feng, Jing-Fei Zhang, and Xin Zhang. Search for sterile neutrinos in a universe of vacuum energy interacting with cold dark matter. *Phys. Dark Univ.*, 23:100261, 2019.
- [79] Lu Feng, Hai-Li Li, Jing-Fei Zhang, and Xin Zhang. Exploring neutrino mass and mass hierarchy in interacting dark energy models. *Sci. China Phys. Mech. Astron.*, 63(2):220401, 2020.
- [80] Hai-Li Li, Lu Feng, Jing-Fei Zhang, and Xin Zhang. Models of vacuum energy interacting with cold dark matter: Constraints and comparison. *Sci. China Phys. Mech. Astron.*, 62(12):120411, 2019.
- [81] Hai-Li Li, Dong-Ze He, Jing-Fei Zhang, and Xin Zhang. Quantifying the impacts of future gravitational-wave data on constraining interacting dark energy. *JCAP*, 06:038, 2020.
- [82] Eleonora Di Valentino, Alessandro Melchiorri, Olga Mena, and Sunny Vagnozzi. Interacting dark energy in the early 2020s: A promising solution to the H_0 and cosmic shear tensions. *Phys. Dark Univ.*, 30:100666, 2020.
- [83] MingMing Zhao, RuiYun Guo, DongZe He, JingFei Zhang, and Xin Zhang. Dark energy versus modified gravity: Impacts on measuring neutrino mass. *Sci. China Phys. Mech. Astron.*, 63(3):230412, 2020.
- [84] Hai-Li Li, Jing-Fei Zhang, and Xin Zhang. Constraints on neutrino mass in the scenario of vacuum energy interacting with cold dark matter after Planck 2018. *Commun. Theor. Phys.*, 72(12):125401, 2020.
- [85] N. Aghanim et al. Planck 2018 results. VI. Cosmological parameters. *Astron. Astrophys.*, 641:A6, 2020.
- [86] N. Kaiser. Clustering in real space and in redshift space. *Mon. Not. Roy. Astron. Soc.*, 227:1–27, 1987.
- [87] Antony Lewis, Anthony Challinor, and Anthony Lasenby. Efficient computation of CMB anisotropies in closed FRW models. *Astrophys. J.*, 538:473–476, 2000.
- [88] David J. Bacon et al. Cosmology with Phase 1 of the Square Kilometre Array: Red Book 2018: Technical specifications and performance forecasts. *Publ. Astron. Soc. Austral.*, 37:e007, 2020.
- [89] Max Tegmark. Measuring cosmological parameters with galaxy surveys. *Phys. Rev. Lett.*, 79:3806–3809, 1997.
- [90] R.E. Smith, J.A. Peacock, A. Jenkins, S.D.M. White, C.S. Frenk, F.R. Pearce, P.A. Thomas, G. Efstathiou, and H.M.P. Couchmann. Stable clustering, the halo model and nonlinear cosmological power spectra. *Mon. Not. Roy. Astron. Soc.*, 341:1311, 2003.
- [91] <http://tianlai.bao.ac.cn>.
- [92] <http://www.jb.man.ac.uk/research/BINGO>.
- [93] <https://fast.bao.ac.cn>.
- [94] <https://www.skatelescope.org>.
- [95] Amadeus Witzemann, Philip Bull, Chris Clarkson,

- Mario G. Santos, Marta Spinelli, and Amanda Weltman. Model-independent curvature determination with 21 cm intensity mapping experiments. *Mon. Not. Roy. Astron. Soc.*, 477(1):L122–L127, 2018.
- [96] Ashley J. Ross, Lado Samushia, Cullan Howlett, Will J. Percival, Angela Burden, and Marc Manera. The clustering of the SDSS DR7 main Galaxy sample – I. A 4 per cent distance measure at $z = 0.15$. *Mon. Not. Roy. Astron. Soc.*, 449(1):835–847, 2015.
- [97] Florian Beutler, Chris Blake, Matthew Colless, D.Heath Jones, Lister Staveley-Smith, Lachlan Campbell, Quentin Parker, Will Saunders, and Fred Watson. The 6dF Galaxy Survey: Baryon Acoustic Oscillations and the Local Hubble Constant. *Mon. Not. Roy. Astron. Soc.*, 416:3017–3032, 2011.
- [98] Shadab Alam et al. The clustering of galaxies in the completed SDSS-III Baryon Oscillation Spectroscopic Survey: cosmological analysis of the DR12 galaxy sample. *Mon. Not. Roy. Astron. Soc.*, 470(3):2617–2652, 2017.
- [99] Wenjuan Fang, Wayne Hu, and Antony Lewis. Crossing the Phantom Divide with Parameterized Post-Friedmann Dark Energy. *Phys. Rev. D*, 78:087303, 2008.
- [100] Antony Lewis and Sarah Bridle. Cosmological parameters from CMB and other data: A Monte Carlo approach. *Phys. Rev. D*, 66:103511, 2002.